NeuroImage 238 (2021) 118160

Contents lists available at ScienceDirect

NeuroImage

journal homepage: www.elsevier.com/locate/neuroimage

Prestimulus dynamics blend with the stimulus in neural variability quenching

Annemarie Wolff[a,‡,*], Liang Chen[e,*], Shankar Tumati[a], Mehrshad Golesorkhi[b], Javier Gomez-Pilar[c,d], Jie Hu[e], Shize Jiang[e], Ying Mao[e], André Longtin[f,g], Georg Northoff[a,f]

[a] University of Ottawa Institute of Mental Health Research, Ottawa, Canada
[b] School of Electrical Engineering and Computer Science, University of Ottawa, Ottawa, Canada
[c] Biomedical Engineering Group, Higher Technical School of Telecommunications Engineering, University of Valladolid, Valladolid, Spain
[d] Centro de Investigación Biomédica en Red—Bioingeniería, Biomateriales y Nanomedicina, (CIBER-BBN), Spain
[e] Department of Neurological Surgery, Huashan Hospital, Fudan University, Wulumuqi Middle Rd, Shanghai, China
[f] Brain and Mind Research Institute, University of Ottawa, Ottawa, Canada
[g] Physics Department, University of Ottawa, Ottawa, Canada

ARTICLE INFO

Keywords:
Dynamics
Prestimulus
Variability
Trial-to-trial variability
Spontaneous activity
Stereoelectroencephalography
State dependence

ABSTRACT

Neural responses to the same stimulus show significant variability over trials, with this variability typically reduced (quenched) after a stimulus is presented. This trial-to-trial variability (TTV) has been much studied, however how this neural variability quenching is influenced by the ongoing dynamics of the prestimulus period is unknown. Utilizing a human intracranial stereo-electroencephalography (sEEG) data set, we investigate how prestimulus dynamics, as operationalized by standard deviation (SD), shapes poststimulus activity through trial-to-trial variability (TTV). We first observed greater poststimulus variability quenching in those real trials exhibiting high prestimulus variability as observed in all frequency bands. Next, we found that the relative effect of the stimulus was higher in the later (300-600ms) than the earlier (0-300ms) poststimulus period. Lastly, we replicate our findings in a separate EEG dataset and extend them by finding that trials with high prestimulus variability in the theta and alpha bands had faster reaction times. Together, our results demonstrate that stimulus-related activity, including its variability, is a blend of two factors: 1) the effects of the external stimulus itself, and 2) the effects of the ongoing dynamics spilling over from the prestimulus period - the state at stimulus onset - with the second dwarfing the influence of the first.

1. Introduction

Over the past ten years, many studies (Baria et al., 2017; Galindo-Leon et al., 2019; He, 2013; Hirschmann et al., 2019; Huang et al., 2017; Nieus et al., 2018; Podvalny et al., 2019) have demonstrated that post-stimulus activity levels depend on the initial state, the level of activity before the stimulus is presented (Benwell et al., 2017; Fellinger et al., 2011; Hanslmayr et al., 2013; He, 2013; Hirschmann et al., 2019; Huang et al., 2017; Mathewson et al., 2009; Milton and Pleydell-Pearce, 2016; Northoff et al., 2010; Yamagishi et al., 2008). Despite these findings, the mechanism of such state-dependence is unclear; how does prestimulus activity shape stimulus-induced activity beyond the effect of the external stimulus?

Variability of the signal may be a key factor. As neural responses to the same stimulus show significant variability over trials (Churchland et al., 2010; He, 2013), the quenching (reduction) of this neural variability occurs after stimulus onset (Arazi et al., 2017a, 2017b; Churchland et al., 2010; Daniel et al., 2019; Haar et al., 2017; Huang et al., 2018, 2017; Schurger et al., 2015), though increases in neural variability have also been observed at multiple levels (Churchland et al., 2011; Haar et al., 2017; Huang et al., 2018; Wolff et al., 2019c). Although much studied, how this neural variability quenching in the poststimulus period - termed trial-to-trial variability (TTV) - is influenced by the prestimulus state is unknown.

TTV describes and indexes (Arazi et al., 2017a, 2017b; Churchland et al., 2010; Ferri et al., 2015; He and Zempel, 2013; Huang et al., 2017; Schurger et al., 2015) the suppression of the variability of the spontaneous brain activity by the arrival of the stimulus (Arazi et al., 2017a, 2017b; Churchland et al., 2011, 2010; Dinstein et al., 2015; He, 2013; He and Zempel, 2013; Wolff et al., 2019c). TTV quenching has been observed on multiple levels of neural activity: cellular (Arieli et al., 1996; Chang et al., 2012; Churchland et al., 2011, 2010; Finn et al.,

* Corresponding authors.
E-mail addresses: awolf037@uottawa.ca (A. Wolff), chenlianghs@126.com (L. Chen).
‡ Lead Contact: awolf037@uottawa.ca.

https://doi.org/10.1016/j.neuroimage.2021.118160.
Received 9 February 2021; Received in revised form 30 April 2021; Accepted 9 May 2021
Available online 28 May 2021.

2007; Goris et al., 2014; Hussar and Pasternak, 2010; Liu et al., 2016; Mazzucato et al., 2016, 2015; Monier et al., 2003; Scaglione et al., 2011; White et al., 2012); scalp-level (Arazi et al., 2017b, 2017a; He and Zempel, 2013; Schurger et al., 2015); functional magnetic resonance imaging (fMRI) (Ferri et al., 2015; He, 2013; Huang et al., 2017) (see also (Dinstein et al., 2015) for review of TTV).

In addition to its varying modulation by different stimuli (Arazi et al., 2017b; Churchland et al., 2011, 2010; Hussar and Pasternak, 2010; Wolff et al., 2019c), previous studies suggest that TTV is also dependent on the degree of the brain's variability at stimulus onset. In non-human data, studies examining prestimulus variability in neural activity have provided direct evidence of its modulating effect on stimulus-related sensory activity (Benwell et al., 2017; Gulbinaite et al., 2017; Hanslmayr et al., 2013; Hennequin et al., 2018; Huang et al., 2019; Lin et al., 2015; Luczak et al., 2013; Mathewson et al., 2009; Romei et al., 2008; Scholvinck et al., 2015; Shimaoka et al., 2019; Yamagishi et al., 2008). Moreover, cell-level studies in animals have shown a strong dependence of poststimulus TTV and behavior (reaction times) on prestimulus variability (Curto et al., 2009; Kisley and Gerstein, 1999; Pachitariu et al., 2015; Schurger et al., 2010). How stimulus related TTV is shaped by prestimulus variability in humans, though, is unknown.

We therefore asked what the electrophysiological relationship in humans is between pre- and poststimulus variability as measured with TTV. Closing the loop between these two factors - variability in humans before (as measured by prestimulus standard deviation (SD)(Garrett et al., 2013; Waschke et al., 2021)) and after stimulus onset (as measured by TTV) – to demonstrate state-dependence of stimulus-induced activity is the aim of the present study.

Specifically, we aimed to investigate how prestimulus activity shapes poststimulus activity, hypothesizing that their interaction is mediated by variability; what is the relationship between pre- and poststimulus variability in humans as measured with TTV? In addressing this question, we encountered the methodological challenge of linking the continuous ongoing dynamics (timepoint-to-timepoint within a single trial) of the prestimulus period to the measurement of discrete, discontinuous (over all trials at a single timepoint) activity time-locked to a stimulus (see (Huk et al., 2018)). To combine both, we introduce a novel methodological strategy by testing whether prestimulus temporal SD, as measured in a continuous way (from timepoint-to-timepoint in each trial) through standard deviation, influences poststimulus variability, measured in a discontinuous way (over trials at a single timepoint) by TTV (Huk et al., 2018) (Fig. 1).

Based on the data described above (Baria et al., 2017; He, 2013; Huang et al., 2017), we had four hypotheses: i) poststimulus TTV in real trials would show more TTV quenching than in pseudotrials (as related to variability in ongoing activity independent of the external stimulus; see below) (thus reflecting the effects of the external stimulus itself independent of the ongoing dynamics); ii) there would be differences in poststimulus TTV between prestimulus low and high SD (reflecting the impact of the ongoing prestimulus dynamics on stimulus-related activity); iii) there would be differences in the impact of prestimulus low and high on TTV quenching in different frequency bands (reflecting differential impact of various frequency bands on pre-poststimulus shaping), specifically in the alpha and beta bands which have previously showed TTV differences (Wolff et al., 2019c); iv) there would be a difference in reaction times between trials with prestimulus low and high in the alpha band (Wolff et al., 2019b) (reflecting the behavioral relevance of the ongoing dynamics).

We addressed these hypotheses by investigating human intracranial electrophysiological activity, which measures local field potentials (LFP) (Buzsáki et al., 2012), as acquired in a stereoelectroencephalography (sEEG) dataset comprised of 20 participants. We applied a simple paradigm with two different stimuli and no behavioral response – a no-report paradigm (Tsuchiya et al., 2015). This allowed us to test the impact of the stimulus alone on stimulus-related activity, independent of any behavioral and cognitive constraints as well as uncontaminated by any response-related neural activity.

Furthermore, we applied the method of pseudotrials (Huang et al., 2017; Wolff et al., 2019c). Pseudotrials (also referred to as surrogate trials He (2013)) describe time periods between stimulus presentation when a stimulus is absent (Dinstein et al., 2015). Used to model the ongoing dynamics of the spontaneous activity, pseudotrials serve as a baseline for the recorded activity when a stimulus was presented (Huang et al., 2017). When the activity during these pseudotrials was subtracted from the activity of the real trials, the difference shows the stimulus-related activity itself, independent of the impact of the ongoing dynamics (Huang et al., 2017). This allowed us to parcel out and distinguish the effects of the external stimulus itself, and those of the prestimulus dynamics, on stimulus-related activity as measured with TTV.

2. Results

Using the methodological factors described above, we set out to test the relationship between prestimulus variability (measured by SD) and poststimulus variability (measured by TTV). With sEEG data, we first calculated the SD (an index of variability) of the signal amplitude in the prestimulus period (varying interval lengths, see methods) (Fig. 1). After a median split, trials were assigned to either the prestimulus low or high SD group (median split) (Fig. 1b). TTV was then calculated in each group in the period after stimulus onset, and the area under the curve was measured.

We then sought to examine the effect of the stimulus, including the timing of its effects, on the ongoing pre-poststimulus variability. This was done by comparing the TTV in real trials to that in pseudotrials. Our findings were replicated in a separate EEG dataset (see Supplementary Results) with a report task (Wolff et al., 2019c, 2019b). Finally, as the task in this dataset required that participants respond behaviorally, we tested whether the shaping of TTV by prestimulus SD is relevant for behavior.

2.1. Prestimulus variability has a significant effect on poststimulus TTV in real and pseudotrials

After verifying the presence (real trials) and absence (pseudotrials) of a stimulus in the event-related potentials (ERPs) (Supplementary Results, Supplementary figure 1a) ($p = 2.536 \times 10^{-4}$), individual trials were sorted according to their prestimulus SD (Fig. 1, Supplementary Fig. 1cd, see methods). Trials with the lowest half of SD were assigned to the prestimulus low group while trials in the top half of the SD were assigned to the prestimulus high group (Fig. 1, Supplementary Figure 1CD).

Once this SD median split had been done, TTV was calculated (Fig. 1 step 4). TTV was defined as the variability changes relative to variability at stimulus onset (see (Arazi et al., 2017a, 2017b; He and Zempel, 2013; Wolff et al., 2019c) for related methods). We calculated the percent change with respect to the value at stimulus onset (Arazi et al., 2017a, 2017b; He, 2013),

$$TTV(t) = \frac{\sigma_{ot}(t) - \sigma_{ot}(0)}{\sigma_{ot}(0)} \times 100 \quad (1)$$

where $\sigma_{ot}(t)$ is the SD of the sEEG signal over trials as function of time t and $\sigma_{ot}(0)$ is the SD over trials at stimulus onset, or 0ms (no difference between SD at stimulus onset between real and pseudotrials with $p = .065$). To determine if there was a difference in the poststimulus activity in the groups split by prestimulus SD, the area under the curve (AUC) between 450 and 550ms was tested (approximate maximum TTV quenching according to Fig. 2c).

In the broadband, a 2 (prestimulus high, prestimulus low) x 2 (real trials, pseudotrials) repeated measures ANOVA found a significant difference in TTV AUC between low and high prestimulus

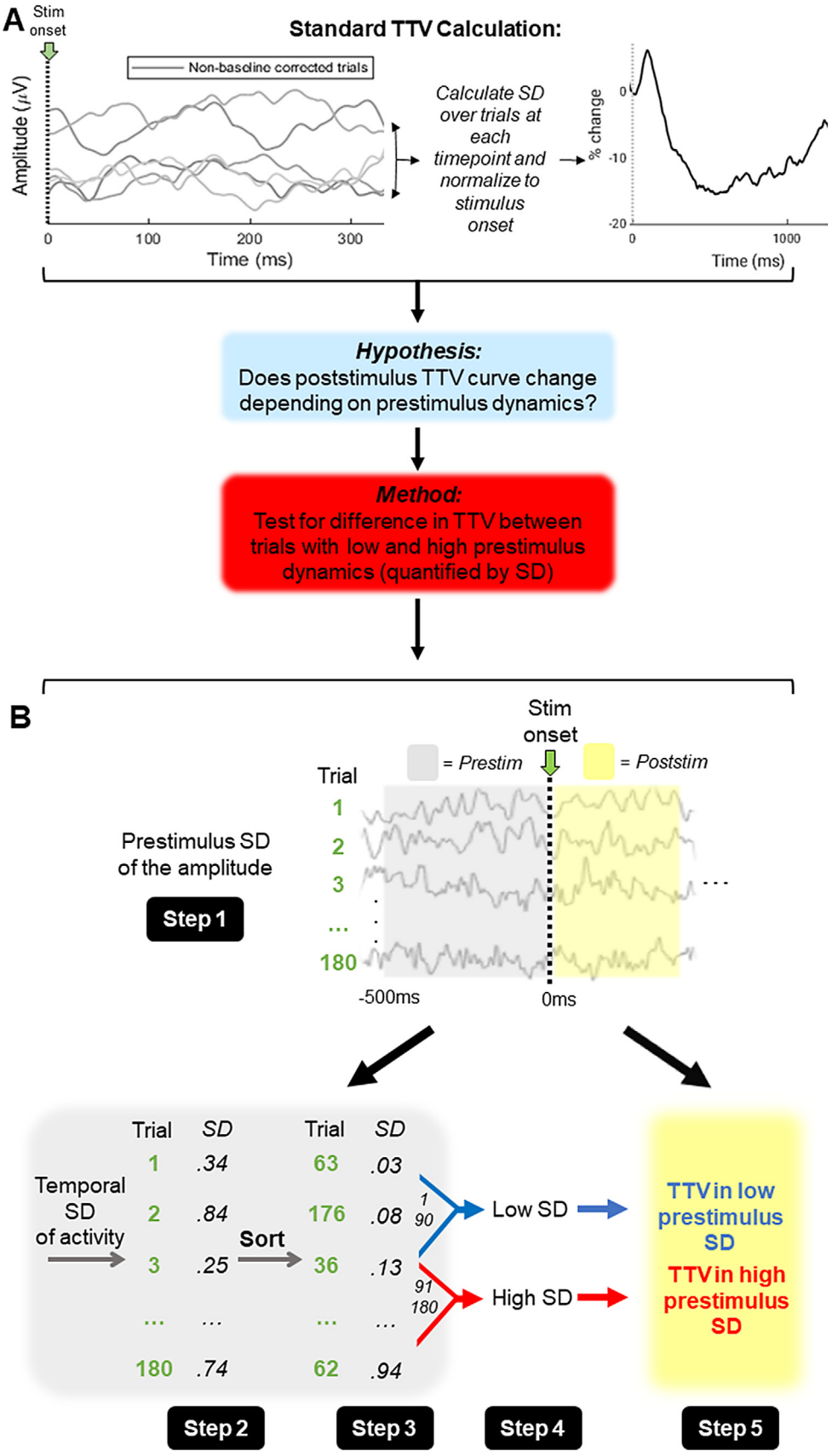

Fig. 1. Standard trial-to-trial variability (TTV) calculation and our adjusted method. A) TTV is usually calculated by determining the standard deviation (SD) at each timepoint over all trials, then normalized by subtracting and dividing by the SD at stimulus onset (time = 0ms). From this standard calculation, our hypothesis and method of the study resulted. B) Calculation of prestimulus SD and sorting of trials into prestimulus low and high. *Step 1* – A window prior to stimulus onset (500ms in the broadband) was chosen for each frequency band. *Step 2* - The standard deviation of the signal amplitude was calculated in each trial. This continuous measure (Huk et al., 2018) yielded one value per trial. *Step 3* – These values were then sorted in ascending order. *Step 4* – As there were 180 trials, after sorting trials 1 to 90 were categorized as prestimulus low SD, while trials 91 to 180 were categorized as prestimulus high SD (median split). *Step 5* – In each group - prestimulus low, prestimulus high - which consists of 90 trials, TTV was calculated according to the methods of (Wolff et al., 2019c). Hereafter, prestimulus low denotes the TTV computed on the trials with the lower prestimulus SD (trials 1-90) while prestimulus high denotes TTV computed on the trials with the higher prestimulus SD (trials 91-180). TTV is a discontinuous measure (Huk et al., 2018) as it is calculated over trials.

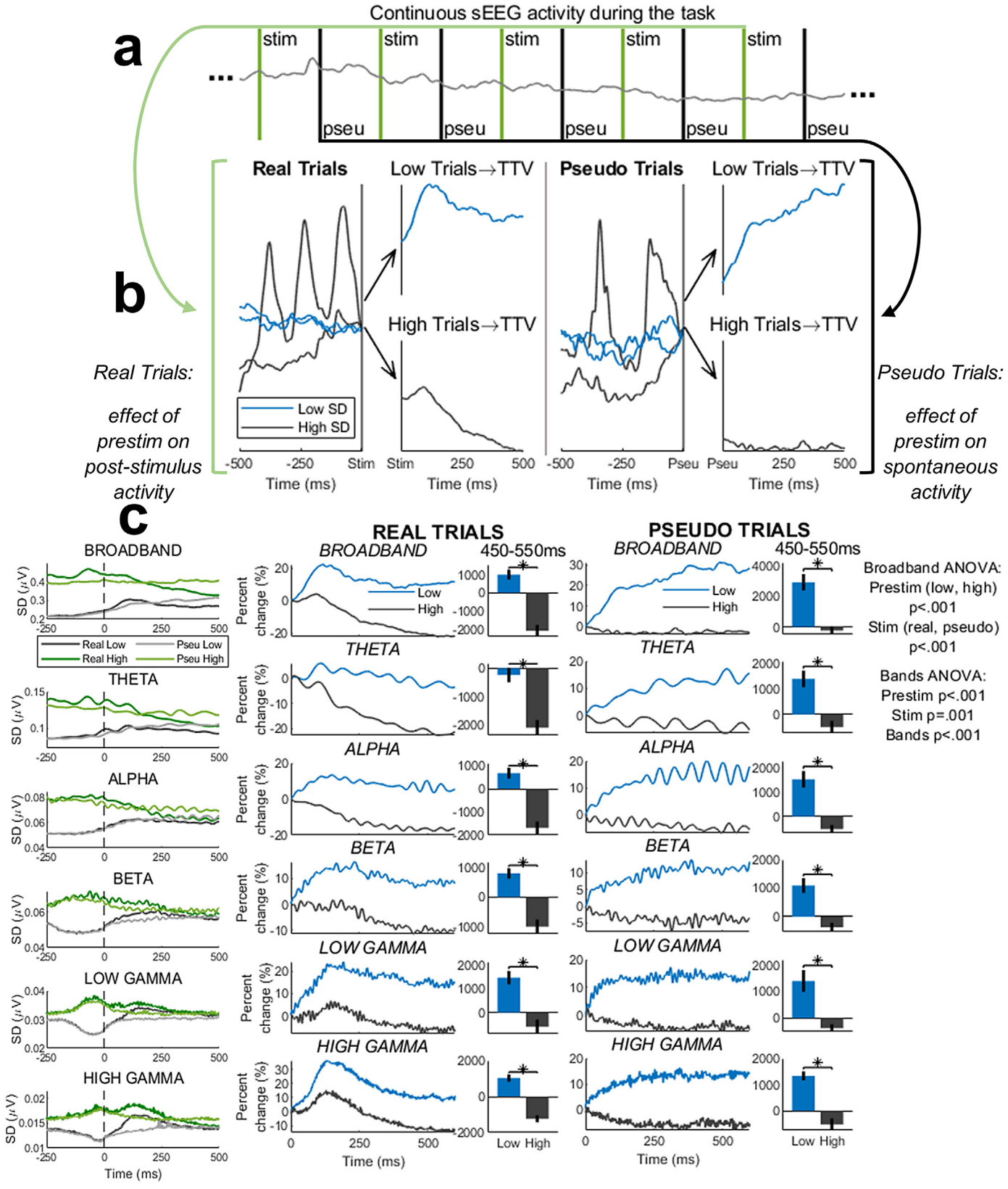

Fig. 2. Trial-to-trial variability (TTV) in real and pseudotrials for all frequency bands. a) Real trials (green lines) were from stimulus onset (0ms) while pseudotrials (black lines) were from a virtual stimulus during the intertrial intervals. b) The standard deviation (SD) from a prestimulus period was calculated to each real and pseudotrial. Those trials with high prestimulus SD were then assigned to the prestim high group, and TTV over all these trials were calculated from them. The same was done for the low prestimulus SD. c) TTV in real trials for prestimulus low and high. *Left column*: Both real and pseudotrials SD over trials (at each timepoint) without the normalization to stimulus onset. *Center and Right column*: Area under the curve (AUC) from 450 to 550ms was calculated and compared (bar plots). TTV in pseudotrials with AUC for the same time interval compared. In the broadband, a 2 (prestimulus low, prestimulus high) x 2 (real trials, pseudotrials) repeated measures ANOVA on the AUC found an effect of prestimulus ($p < .001$) and stimulus ($p < .001$). In all bands, a 2 (prestimulus low, prestimulus high) x 2 (real trials, pseudotrials) x 5 (bands) repeated measures ANOVA found effects of prestimulus ($p < .001$), stimulus ($p = .001$), and bands ($p < .001$). Gray shaded areas are interval of calculation of AUC which is shown in the bar plots. Error bars show standard error. Each curve/bar is the mean of all participants.

($F(1,19) = 58.692$, $p < .001$ $\eta_p^2 = .755$) and between real and pseudotrials ($F(1,19) = 30.294$, $p < .001$, $\eta_p^2 = .615$) (Fig. 2c). There was a large effect size for both factors.

Next, to measure the same factors in the individual frequency bands, a 2 (prestimulus low, prestimulus high) x 2 (real trials, pseudotrials) x 5 (theta, alpha, beta, low gamma, high gamma) repeated measures ANOVA was done. As in the broadband, there was a significant effect in TTV AUC of prestimulus ($F(1,19) = 39.288$, $p < .001$, $\eta_p^2 = .674$), trials ($F(1,19) = 14.400$, $p = .001$, $\eta_p^2 = .431$) and frequency bands ($F(2.495, 47.402) = 16.132$, Greenhouse-Geisser corrected $p < .001$, $\eta_p^2 = .459$), with a large effect size in all three factors. After these results, the impact of the interval of the prestimulus SD was examined (see Supplementary Results). With one prestimulus interval longer than that used above, and one shorter, no significant effect of window size was found (Supplementary Tables 3–5).

Together our results show the effect of prestimulus variability on TTV: the level of prestimulus SD exerts a strong impact on poststimulus variability in both real and pseudotrials. More generally, our well-controlled findings show the strong degree to which intrinsic prestimulus SD shapes poststimulus activity, in addition to the effect of the external stimulus.

2.1.1. Poststimulus TTV disambiguates the effect of the stimulus from the ongoing spontaneous activity

Since our results above showed a similar difference between prestimulus low and high in pseudotrials as in real trials, we wanted to investigate the effect of the stimulus itself on poststimulus TTV.

Measured neural activity after stimulus onset, A_m, is a sum of multiple activities, plus their interaction (He, 2013; Huang et al., 2017):

$$A_m(t) = A_o(t) + A_s(t) + I_{o,s}(t) \quad (3)$$

where A_o is the ongoing spontaneous activity at timepoint t, A_s is the stimulus-related activity, and $I_{o,s}$ is the interaction between the ongoing spontaneous activity and the stimulus-related activity. As it is not possible to measure the interaction between A_o and A_s ($I_{o,s}$) directly - A_o continues to change after stimulus onset He (2013) – neural activity was replaced with variability over trials (TTV) in order to isolate stimulus-related activity (A_s). TTV encompasses the interaction of the ongoing spontaneous activity with the stimulus-related activity ($I_{o,s}$) within it; it is measured relative to SD at stimulus onset and measures the variability over trials. Therefore, to account for this interaction, the neural activity was replaced by the variability over trials, or TTV:

$$TTV_r(t) = TTV_p(t) + TTV_s(t) \quad (4)$$

where TTV_r is the TTV measured in the real trials at timepoint t, TTV_p is the TTV of the ongoing spontaneous activity as measured in the pseudotrials, and TTV_s is the TTV of the stimulus-related activity (correlations are neglected).

To isolate the effect of the stimulus, the broadband TTV in real and pseudotrials were compared separately for prestimulus low and high (Fig. 2c). For each timepoint from stim onset (0ms) to 600ms, two repeated measures t-tests were calculated with the respective TTV for all participants. The two tests were a) prestimulus low in real trials compared to prestimulus low in pseudotrials, and b) prestimulus high in real trials compared to prestimulus high in pseudotrials. Therefore, the TTV at timepoint one for all participants (20 patients) in real trials was tested against the TTV at the same timepoint for all participants in pseudotrials. As this was done at each timepoint, it produced a timeseries of p-values, as was done previously He and Zempel (2013).

This p-value timeseries was then corrected for multiple comparisons Benjamini and Hochberg (1995) and plotted (Fig. 3a). The time interval when the corrected p-value timeseries was less than .05 was considered the interval during which the stimulus had an impact. We considered it so as there was a significant difference between the TTV when a stimulus was presented and the TTV when no stimulus was presented; we considered the stimulus to have an impact when there was a difference between the real trials and the pseudotrials. In prestimulus low, this timepoint was found to be at 226 ms, while the significance level was passed at 254 ms in prestimulus high.

Table 1
TTV AUC 2 × 2 repeated measures ANOVA in broadband for all trials.

Factor	Levels	df	F - value	p - value	η_p^2
Trials	Real, Pseudo	1, 19	9.649	.006	.337
Interval	Early, Late		16.601	.001	.466
Interaction			6.402	.020	.252

df = degrees of freedom
ηp2 = partial eta squared

After visualizing the resulting p-value timeseries', they crossed the significance level at slightly before the 300 ms mark, or the halfway point of our poststimulus window. Therefore, the stimulus was considered to have a significant impact on the TTV after the points where the p-value timeseries crossed this significant threshold.

To verify our finding above in a second way, we divided the poststimulus window into two equal intervals (300 timepoints), an earlier one and a later one (henceforth termed 'early' and 'late'). To determine the effect of prestimulus variability and trials (real, pseudotrials) in these two intervals (early: 0-300ms, late: 300-600ms), the AUC during the two intervals for each of the four TTV curves were compared (Fig. 3b). In the early time interval, a 2 (prestimulus low, prestimulus high) x 2 (real trials, pseudotrials) repeated measures ANOVA found a significant effect of prestimulus ($F(1,19) = 56.291$, $p < .001$, $\eta_p^2 = .748$) but not of stimulus ($F(1,19) = .896$, $p = .356$, $\eta_p^2 = .045$). In contrast, the late time interval found a significant effect of both prestimulus ($F(1,19) = 60.795$, $p < .001$, $\eta_p^2 = .762$) and stimulus ($F(1,19) = 39.402$, $p < .001$, $\eta_p^2 = .675$).

Next, to isolate the stimulus-related variability quenching (TTV reduction), Eq. 4 must be rearranged:

$$TTV_s(t) = TTV_r(t) - TTV_p(t) \quad (5)$$

We did this by subtracting the TTV curves at each timepoint t in the pseudotrials (TTV_p) from that in the real trials (TTV_r) in the two time intervals (Fig. 3b). These TTV curves were titled 'corrected TTV' (cTTV) as the subtraction of the pseudotrials removed - corrected for - the effect of the prestimulus variability.

The AUC of the resulting curves were calculated, and the absolute value was taken (only the magnitude was of interest, not whether the TTV curve increased or decreased in variability). This allowed us to isolate the change in variability due to the stimulus; it is hypothesized that subtracting the pseudotrials effectively removes the variability related to the ongoing activity (He, 2013; Huang et al., 2017).

A 2 (prestimulus low, prestimulus high) x 2 (early, late) repeated measures ANOVA found no significant effect of prestimulus SD ($F(1,19) = .289$, $p = .597$, $\eta_p^2 = .015$) and a significant effect of time interval ($F(1,19) = 19.305$, $p < .001$, $\eta_p^2 = .504$).

Finally, in the same early and late time intervals, the TTV AUC for all real and pseudotrials (prestimulus low and high together) was measured (Fig. 3c). This was done to measure the effect of the stimulus only on poststimulus variability. For this reason, the trials were not divided according to prestimulus variability as its effect had been examined above. The factor being measured was the effect of the stimulus, so the comparison between real trials (had a stimulus) and pseudotrials (stimulus was absent) was done here. A 2 (real trials, pseudotrials) x 2 (early, late) repeated measures ANOVA found a significant effect of both stimulus and time interval, and a significant interaction between the two factors (Fig. 3de, Table 1).

These findings show the effect of the stimulus itself on poststimulus variability in two ways. They indicate that the early period of poststimulus activity – 0-300 ms - is shaped by both the state-dependent variability of prestimulus SD and the external stimulus. In the later period

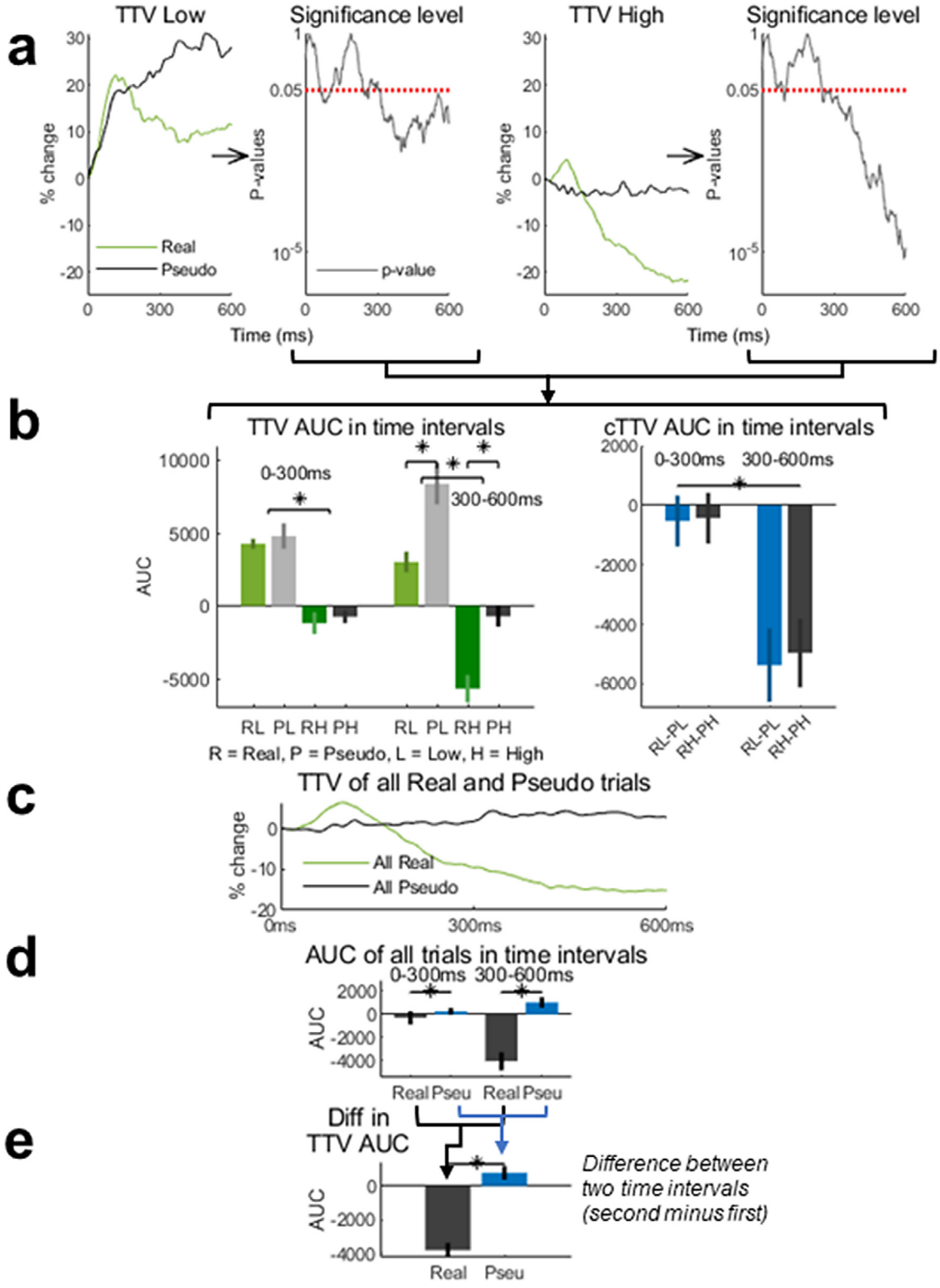

Fig. 3. Effect of stimulus on trial-to-trial variability. a) Broadband trial-to-trial variability (TTV) in real and pseudotrials. Each curve is the mean of all participants. To determine the effect of the stimulus, repeated measures *t*-tests were done for all data points between the broadband TTV of real and pseudotrials shown in a. The *p*-values – Benjamini-Hochberg corrected for multiple comparisons – were then plotted for all timepoints. The *p*-values fell below the significance level (.05) just before 300ms. b) After the findings in *a*, the poststimulus period was divided into two equal intervals, 0-300ms and 300-600ms. The area under the curve (AUC) was then calculated for all TTV curves in a for both intervals. 2 × 2 repeated measures ANOVAs in each interval found an effect of prestimulus only in the early intervals, and of prestimulus and stimulus in the late interval. Right plot: For each timepoint the TTV curve for the pseudotrial was subtracted from that of the real trial. The AUC was then calculated, and a 2 × 2 repeated measures ANOVA was done to determine the effect of prestimulus and time interval. No effect of prestimulus was found, though an effect of time interval was. c) TTV in all real trials and all pseudotrials. d) Finally, in the same intervals from *b*, the AUC for TTV in all trials – not divided by prestimulus low and high – and pseudotrials was compared. An effect of time interval was found, as was stimulus (real and pseudo). e) Finally, the difference between the two intervals was calculated, and a significant difference was found. Each bar is the mean of all participants.

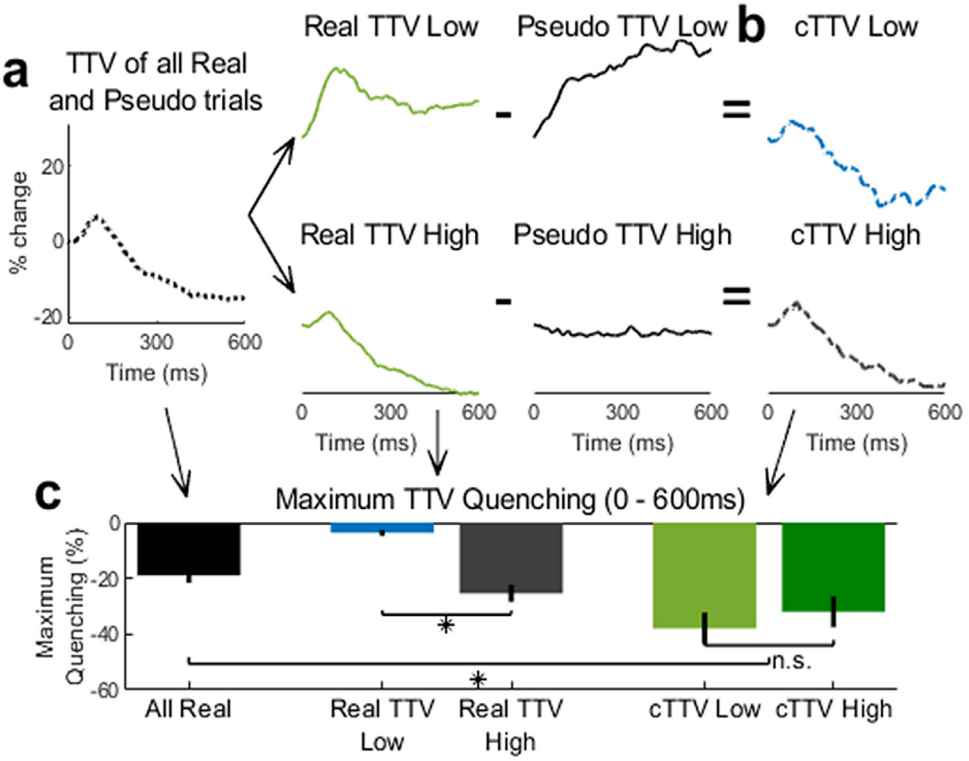

Fig. 4. Corrected trial-to-trial variability (cTTV) and its maximum quenching. a) cTTV (*b*) is equal to TTV of real trials minus TTV of pseudotrials – for prestimulus low and high. c) TTV maximum quenching (0–600 ms) for all trials, TTV and cTTV. In all real trials (black bar, left), max quenching is less than 20%. When the trials are divided into prestimulus low and high (blue and gray bars, center), the maximum quenching differs between them. When cTTV is calculated, therefore corrected for prestimulus effects by subtracting pseudotrials (*b*), maximum quenching no longer differs between prestimulus low and high (green bars, right), though does differ from that of TTV in all real trials (black bar, left). Each curve/bar is the mean of all participants.

– 300–600 ms - the external stimulus exerts a relatively stronger impact on poststimulus activity than the ongoing spontaneous variability.

2.2. Poststimulus TTV corrected for prestimulus variability shows greater quenching than uncorrected TTV

To this point, we found that prestimulus variability has a significant impact on poststimulus variability. Based on these findings, we next hypothesized that if the TTV curves were corrected for prestimulus variability, the poststimulus differences between prestimulus low and high would decrease, and the magnitude of the TTV quenching would increase. As the difference in poststimulus variability was due to prestimulus variability if we were to remove this factor – prestimulus variability – the resulting difference after stimulus onset should therefore be gone. This would be possible using pseudotrials as they serve as a model for the ongoing spontaneous activity when no stimulus is present (Huang et al., 2017; Wolff et al., 2019c).

We therefore tested this by calculating TTV corrected using pseudotrials (cTTV),

$$cTTV(t) = TTV_r(t) - TTV_p(t) \quad (5)$$

with TTV_r being the curve of the real trials, TTV_p being the curve of the pseudotrials, and t being the data point in the timeseries ($0 \leq t \leq 600$). The poststimulus variability of the real trials would have the effect of their prestimulus variability removed by subtracting the poststimulus variability of the pseudotrials; the pseudotrials contain only the effect of the prestimulus variability.

The maximum quenching (percent change) between stimulus onset and 600 ms was measured for three groups of trials: 1) all real trials together (180 trials per curve Fig. 4ac far left bar); 2) real trials divided into prestimulus low and prestimulus high (90 trials per curve, Fig. 4ac center two bars); 3) corrected TTV (cTTV) – real trials TTV minus pseudotrials TTV - divided by prestimulus low and prestimulus high (90 trials per curve, Fig. 4bc right two bars). All trials together show poststimulus variability when prestimulus variability is ignored, separated by prestimulus variability shows its effect on poststimulus variability, and corrected maximum quenching shows the effect on poststimulus variability when prestimulus variability is accounted for and removed.

Table 2
sEEG Maximum sEEG quenching in TTV and cTTV repeated measures t-test results.

Curve	Prestimulus	Mean	*t*-value	*p*-value
TTV	Low	-3.69 ± 4.39	6.79*	1.430×10^{-7}†
	High	-25.35 ± 13.20		
cTTV	Low	-37.94 ± 24.59	-0.77*	.449†
	High	-31.92 ± 23.84		

* = Degrees of freedom are 38
† = False Discovery Rate corrected

Table 3
Maximum sEEG quenching between TTV and cTTV in all trials repeated measures *t*-test results.

Curve for all trials	Mean	*t*-value	*p*-value
TTV	-18.96 ± 11.38	3.23*	.004†
cTTV	-34.93 ± 18.94		

* = Degrees of freedom are 38
† = False Discovery Rate corrected

Our results supported our hypothesis. A repeated measures *t*-test (participants provided data to both levels) found a significant difference in the maximum quenching in TTV, but not cTTV (Table 2). The difference in quenching between prestimulus low and high disappeared when TTV was corrected for prestimulus SD.

Lastly, to compare quenching in TTV to cTTV when all trials were combined (180 trials), the maximum quenching in these two curves was measured. A repeated measures *t*-test found a significant difference between TTV (Fig. 4c center two bars) and cTTV (Fig. 4c right two bars) maximum quenching (Table 3), with greater quenching in the cTTV.

Finally, to replicate our TTV and cTTV findings in the sEEG data, we did the same analysis (with standard EEG preprocessing) (see Supple-

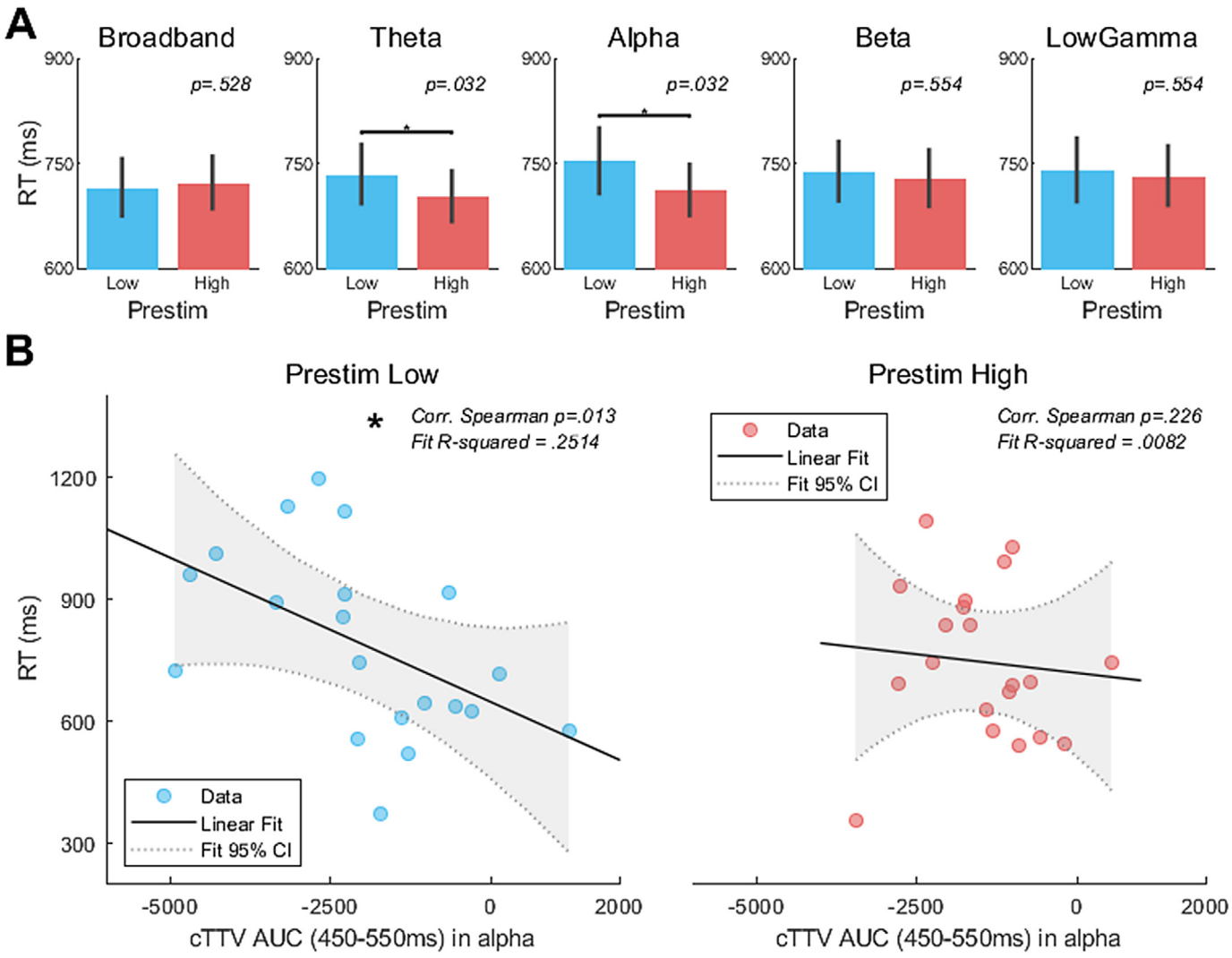

Fig. 5. Behavioral relevance of prestimulus SD shown in EEG dataset. A) Real trials in each frequency band were split into thirds based on the prestimulus SD and the reaction times for the top and bottom third were extracted. The mean was calculated. A repeated measures *t*-test was done to compare the mean reaction times of prestimulus low and high. There was a significant effect of prestimulus SD in the theta and alpha bands (p = .032, .032, Benjamini-Hochberg FDR corrected). Each bar is the mean of all participants. B) In these two bands only, the TTV AUC (450-550ms) was Pearson correlated with mean reaction times. In the alpha band, the TTV AUC of prestimulus low had a significant correlation with mean reaction time (p = .013), but the prestimulus high did not (p = .226).

mentary Results). We found the same results, with greater quenching in the cTTV data than in the TTV data calculated in the standard way.

2.3. In sum, these findings show that correction for prestimulus SD and its ongoing variability yields larger TTV quenching when compared to TTV measured in the standard way, with no correction

2.3.1. Significant effect of prestimulus variability on reaction times in the theta and alpha frequency bands

Finally, we wanted to determine if there was behavioral relevance for prestimulus variability, and if reaction times correlated with post-stimulus TTV. With the EEG data used for replication (see Supplementary Results), the mean reaction time from the trials with the lowest and highest third (bottom and top 60 trials) of prestimulus variability was calculated for the broadband and each frequency band (Fig. 5a).

Repeated measures *t*-tests found a significant difference in the mean reaction times in the theta ($t(19)$ = 2.31, p = .032) and alpha ($t(19)$ = 2.59, p = .032) bands. There was no significant difference in the broadband, beta, and low gamma bands (p = .528, .554, .494 respectively).

Next, to correlate the standard TTV AUC measured (see Supplementary Figure 5 and Results) in these two significant frequency bands (theta, alpha) with the mean reaction times, two-tailed Spearman correlations were done. None of the correlations were significant (theta: p_{low} = .191 and p_{high} = .191; alpha: p_{low} = .264 and p_{high} = .273).

However, when the same correlations were done between the AUC from the cTTV (Supplementary Fig. 6) and the reaction times, the correlation was significant between the alpha band and the prestimulus low group (r = -.597, p = .013, linear fit R-squared = .2514, linear fit sum of squares due to error = 7.278×10^5) (Fig. 5b). This was not significant in the prestimulus high group (r = -.597, p = .013, linear fit R-squared = .0082, linear fit sum of squares due to error = 6.745×10^5) or either of the theta correlations (p_{low} = .581 and p_{high} = .130).

Finally, to test whether 1) the correlation between cTTV AUC and reaction time were significantly different in prestimulus low and high, and 2) whether these correlations were different between cTTV AUC and regular TTV AUC, Fisher's *r*-to-*z* transformation was done (He et al., 2008). This found that there was a difference between prestimulus low and prestimulus high in the correlation with reaction time and cTTV

AUC (p = .246), and a difference in the correlations between reaction time of cTTV and TTV (p_{low} = .344, p_{high} = .936).

In sum, we show that prestimulus SD not only shapes poststimulus activity, but also associated behavior in a complex cognitive task, especially in the alpha band.

3. Discussion

We investigate the impact of the ongoing dynamics, e.g. prestimulus SD, on poststimulus activity as measured with TTV in intracranial electrophysiological recordings (sEEG). First, we show that prestimulus SD impacts poststimulus activity in real trials as we observed differences in the latter between prestimulus high and low trials. This served as a basis for our second main finding: the late poststimulus period (300-600ms) shows a greater impact of the external stimulus (relative to the ongoing dynamics) than the early poststimulus period (0-300ms) (where the impact of the ongoing dynamics dominates).

Next, we found that when corrected for prestimulus SD – subtracting the TTV of the pseudotrials from the TTV of the real trials - the maximum quenching of poststimulus variability was the same in trials with low or high prestimulus variability; this reflects the impact of the external stimulus itself independent of the ongoing dynamics. In contrast, that was not the case when TTV calculation was not controlled for prestimulus variability, that is, standard TTV curves. This indicates the relevance of accounting for prestimulus SD in the analyses of stimulus-related activity when averaging over trials; controlling for the ongoing prestimulus dynamics is thus key in isolating the effect of the stimulus itself.

Finally, we replicate all sEEG findings in a separate scalp-recorded EEG dataset (Wolff et al., 2019c) with a report paradigm (Tsuchiya et al., 2015). This also allowed us to show the behavioral relevance of prepoststimulus variability, specifically in the alpha band, by shaping reaction time.

Together, the main result of our study is that stimulus-related activity is highly dynamic as it blends and is composed of two components: 1) activity evoked by the stimulus, therefore from an external source; 2) the ongoing dynamics, i.e., variability carrying over from the prestimulus period to the poststimulus period. This carries major implications for our understanding of stimulus-related activity as we show that the influence of the ongoing dynamics dwarfs the influence of the stimulus itself.

3.1. Poststimulus trial-to-trial variability is relative to the ongoing dynamics and the stimulus, especially in the later period

Our finding of a difference in TTV between real trials with prestimulus low and high variability is consistent with previous studies (He, 2013; Huang et al., 2017); activity at stimulus onset, either high or low, has a differential impact on poststimulus activity. We extend these findings by showing that this difference was found not only in the real trials, but also in the pseudotrials when no stimulus is present. The difference found in the pseudotrials is strong evidence of the effect of the ongoing dynamics on poststimulus activity.

The earlier period (0–300 ms) in stimulus-related activity saw a greater influence of the ongoing prestimulus variability than the external stimulus, as seen in Fig. 3bde. The difference in TTV between low and high prestimulus was significant in this early period while the difference between real and pseudo was not. This changed in the later time interval; there were significant differences between both low and high prestimulus, and real and pseudotrials. Of note, differences between real and pseudotrials were slightly different in the prestim low compared to high trials. This difference should be the sole aim of a future paper, but it does support previous findings on nonadditive interactions of the prestimulus state on the poststimulus activity (He, 2013; Huang et al., 2017).

Again, as done above, when the real trials were corrected for prestimulus SD using pseudotrials in this context, the early interval difference between low and high prestimulus disappeared. It also did in the later interval. This last finding again supports our idea of the substantial impact of the prestimulus dynamics as measured with SD on poststimulus activity. While the findings in Fig. 3 show the different temporal course of both prestimulus SD and the external stimulus in shaping stimulus-related activity, the later poststimulus period (300–600 ms) shows a larger impact of the stimulus on TTV compared to the earlier period (before 300 ms).

Together, we demonstrate that the two components identified as shaping poststimulus-induced activity - ongoing dynamics and the external stimulus - differ in their temporal course. The ongoing variability exerts stronger effects in the early period while the impact of the external stimulus is stronger in the later period. It remains to be seen whether the time course of the external stimulus is modulated by diverse stimuli or cognitive requirements related to the said stimulus; this should be a focus of future studies.

3.2. Neurophysiological substrate of prestimulus and its ongoing variability

SEEG recordings acquire the activity of local field potentials (LFPs), which measure membrane-potential derived fluctuations in the extracellular space (Buzsáki et al., 2012). Changes in the LFP of the brain have been shown to be mediated by synchronization after action potential burst hyperpolarization – a burst of fast neuronal spikes is often followed by the hyperpolarization of the membrane - which can be large and contribute to the extracellular field (Pachitariu et al., 2015).

A relevant study of LFPs in gerbils (Pachitariu et al., 2015) found that in desynchronized cortical states low frequency fluctuations are suppressed. This, in turn, allows individual neurons to spike independently with measured activity being more reliable and consistent over trials, and responses to stimuli being faster than in synchronized states. In contrast, in a synchronized cortical state the extracellular space shows strong low frequency LFPs fluctuations with high variability in activity over trials and slower responses to stimuli than in the desynchronized state.

These results on the population level are consistent with ours on a more macroscale. Using sEEG, we, as in their study, measured LFPs which, together with their cellular and population observations, provides a neurophysiological basis for our findings on a wider level. What they described as the desynchronized state in their population-based LFPs corresponds to our more macroscale-based high prestimulus variability; it is associated with stronger poststimulus TTV quenching over trials and faster reaction times in the theta and alpha bands. Similarly, their synchronized state finds its equivalent on the more macroscale level in our prestimulus low variability which had less TTV quenching and slower reactions times. Due to such correspondence, we infer that, on a cellular level, our high prestimulus variability possibly reflects a desynchronized state that exhibits a higher degree of independent spiking and firing of individual neurons, in comparison to the low prestimulus synchronized state. This inference remains tentative, however, and requires a combined investigation of population firing rates and LFPs in humans.

3.3. Limitations

Firstly, though sEEG electrodes are placed in different locations and regions of the brain, we here did not explicitly analyse the spatial and regional differences. We could observe regional differences in TTV which were largely in accordance with previous data (He 2013, Huang et al. 2017). However, as the placement of electrodes in sEEG were dependent upon the pathology of the individual patient (epileptic focus), we here refrained from analyzing the spatial distribution and differences in a more pronounced way.

Secondly, it should be mentioned that Arazi *et al* (Arazi et al., 2017a) observed the TTV peak to be slightly earlier - between 200 and 400 ms after stimulus onset - than the TTV peak in the current dataset which

occurred between 500ms to 800 ms. Though it cannot be verified here, it may be related to differences in stimulus type and length; they presented short visual stimuli for roughly 100ms while we presented verbal stimuli lasting for about 700ms in the sEEG data and long (2s) complex visual stimuli with responses in the replication EEG data.

Thirdly, the prestimulus SD impact on poststimulus activity may have a more cognitive rather than dynamic interpretation, as has been shown in recent studies (Groot et al., 2021; Madore et al., 2020). For instance, one may assume that prestimulus SD reflects the prediction or anticipation of the upcoming stimulus as is consistent with predictive coding Friston (2010) and recent results on prestimulus alpha (Cao et al., 2017). However, our sEEG no-report paradigm did not include any self-generation of the stimuli and presented self and non-self stimuli randomly and with a jitter. This makes any prediction or anticipation (predictive coding) in the prestimulus period unlikely. Therefore, we assume that the prestimulus SD and its impact on poststimulus TTV are more dynamic than cognitive in nature.

4. Conclusion

To address how the ongoing prestimulus dynamics impact the effect of the external stimulus, we investigate the impact of prestimulus SD on poststimulus TTV in an intracranial sEEG data set. Our pre-poststimulus variability analyses found two main findings: 1) poststimulus variability reduction, e.g. TTV quenching, is stimulus-driven and relative to the prestimulus dynamics, as measured through prestimulus variability; 2) the effect of the stimulus is higher in the later poststimulus period (300–600 ms) than the earlier (0–300 ms) where the prestimulus dynamics influence dominates. These results were replicated in a separate EEG dataset and task, which also found that real trials with high prestimulus variability in the theta and alpha bands had faster reaction times. Our findings show that stimulus-related activity is blended, being composed of a) the effects of the external stimulus, and b) the effects of the internal ongoing spontaneous variability, with the second dwarfing the influence of the first.

5. Methods

5.1. sEEG data and analyses

5.1.1. Experimental paradigm

The experimental paradigm presented to the patients was comprised of two auditory stimuli: the subjects' own name and a paired unknown person's name (in their native language, Chinese) are spoken by the same familiar voice (Huang et al., 2018; Lipsman et al., 2014; Qin et al., 2012). The duration of each name was less than 800 ms. The average Root Mean Square (RMS) decibel level was less than -20 dB, with the maximum RMS difference between the two names less than 1 dB. During this no-report paradigm, participants were presented with 180 trials in total, 90 with their own name and the same number of another name. The intertrial interval (ITI) between trials was 3–3.75 s, randomly jittered by 0.25 s – this allowed us to minimize anticipation or prediction effects in our analysis of stimulus-related activity as to focus on its dynamic rather than cognitive components.

5.1.2. Prestimulus SD

Temporal variability as defined here is the moment-to-moment change in a neural signal (Garrett et al., 2013), which in this paper is the timepoint-to-timepoint change. Temporal signal variability measures the distributional width of the timepoints (Garrett et al., 2013; Waschke et al., 2021).

As our aim of the paper was to examine the relationship between pre- and poststimulus variability, with poststimulus variability measured by trial-to-trial variability (TTV), we needed an appropriate measure of prestimulus variability. TTV is calculated in the time-domain (standard deviation at each timepoint across all trials), so our prestim temporal variability measure should likewise be in the time domain. The most simple and widely known of these measures was standard deviation according to the literature (Garrett et al., 2013), so we chose standard deviation.

The SD was calculated according to Eq. 2, then SD values were sorted in ascending order – the first trial had the lowest prestimulus SD, the last trial had the highest - and the median value was calculated (Fig. 1 step 3). Trials below the median were assigned to the low prestimulus group and those above the median to the high prestimulus group, with 90 trials in each.

The time interval for the prestimulus variability calculation varied according to frequency band due to the various period lengths of each band. They were: broadband = -500 to 0 ms; theta = -1000 to 0 ms; alpha = -400 to 0 ms; beta = -200 to 0 ms; low gamma = -100 to 0 ms; high gamma = -50 to 0 ms. To ensure that this window did not affect the results in the TTV AUC, two alternate windows were also calculated and the TTV AUC computed and statistically tested (Table 1).

5.2. sEEG data and analyses

5.2.1. Subjects

Twenty patients (25.13 ± 5.57 years; mean ± SD; 8 female) with drug-resistant epilepsy who underwent sEEG exploration in the department of Neurosurgery of Huashan Hospital (Shanghai, China) from September 2016 to May 2017 were included in this study. SEEG is a long-established invasive evaluation method for patients with drug-resistant epilepsies (Parvizi and Kastner, 2018). All patients had comprehensive presurgical evaluations, including a detailed medical history, scalp EEG, magnetic resonance imaging (MRI), and positron emission tomography (PET) scans prior to sEEG exploration. The choice of the anatomical location of electrodes was based on results from the presurgical evaluation and was made by a team of clinicians independent of the present study.

The study was approved by the research ethics committee of Huashan Hospital, at Fudan University, and all aspects of the study were performed according to their relevant guidelines and regulations. Written informed consent was obtained from the patients, or their guardians, for participation in this study.

5.2.1.1. sEEG recording. The surgical plans were made by stereotactic neuronavigational software (iPlan Cranial 2.0, Brainlab AG) and the procedures were carried out as previously documented (Gonzalez-Martinez, 2016). Double dosage enhanced T1 images were obtained to identify the blood vessels first then the Leksell stereotactic frame (Elekta) was applied to localize the coordinates of the electrodes. Intracerebral multiple contacts electrodes (HKHS, Beijing, China), with a diameter of 0.8 mm and 8–16 contacts, were applied during the surgery which was performed under local anesthesia. The length of each contact was 2 mm with 1.5 mm between contacts. Post-implantation CT scans were performed the day after implantation surgery to 1) exclude intracranial hematoma, and 2) localize the location of each contact.

The sEEG signals were recorded on a Nihon Kohden 256-channel EEG system (EEG-1200C) with a sampling rate of either 1 or 2 kHz, and hardware filtered between 0.01 Hz and 600 Hz. The signals during recording were referenced to white matter in the brain which was defined by the clinicians.

SEEG is minimally contaminated by artifacts such as swallowing, eye movement, muscle movement, etc., compared to scalp EEG, so it is not prone to artifacts related to gaze position, electrode offset variability, and movement (Parvizi and Kastner, 2018) (see for instance Arazi et al. 2017a and b for excellent control of those factors in EEG). This makes sEEG an ideal tool to record and measure specific variability measures such as TTV.

5.2.2. Electrodes localization

Electrodes were auto segmented from post-implanted computed tomography (CT) images (Qin et al., 2017). The post-implantation CT was aligned to preoperative MRI images and contacts were calculated and reconstructed. The locations of these contacts were checked manually with neuronavigational software. Finally, the contacts were labeled based on Freesurfer's parcellation of the MRI.

5.2.3. sEEG preprocessing

Before any data analysis was performed, the timeseries of each contact was examined by an epileptologist who classified contacts as either seizure or non-seizure. To start, as the data for some of the participants was recorded at a sampling rate of 2 kHz while others were recorded at 1kHz, all the former were resampled to 1 kHz using MATLAB's *resample* function which includes an anti-aliasing filter. The events for the task were then imported, superfluous channels (ECG, EMG, etc) were removed, and the contacts previously determined to be seizure contacts by the epileptologist were also removed.

To follow the preprocessing steps of the literature closely, the same methods of two recent sEEG publications (Daitch and Parvizi, 2018; Helfrich et al., 2018), were followed exactly. In MATLAB (The MathWorks, v2012) and according to the methods of Daitch (Daitch and Parvizi, 2018), we calculated the power spectrum for each contact as well as the mean power over all contacts. If the mean power of a given contact was $\geq \pm 5$ SDs of the mean power across all contacts for a given participant, that contact was removed from the data (median = 2 ± 1.2, range = 0–5).

Next, the remaining contacts were two-way zero-phase FIR notch filtered at 50Hz and harmonics (100 Hz, 150 Hz), and rereferenced to the mean of all remaining contacts. The signal was then bandpass filtered using a two-way, zero-phase FIR non-aliasing filter in the following bands: 0.1–1 Hz, 1–4 Hz, 4–8 Hz, 8–13 Hz, 13–30 Hz, 30–70 Hz, 70–80 Hz, 80–90 Hz, 90–100 Hz, 100–110 Hz, 110–120 Hz, 120–130 Hz, 130–140 Hz, 140–150 Hz, 150–160 Hz, 160–170 Hz, and 170–180 Hz.

The instantaneous amplitude for each band was then computed by applying the Hilbert transform (MATLAB function *hilbert*) and taking its modulus. Each datapoint for each contact was then normalized by the mean activity of each contact to partially correct for the $1/f$ nature of electrophysiological signals. The signal for each band was then recombined into one signal by taking the mean of all bands per timepoint per contact.

5.2.4. Event-related potentials confirm neural response to stimuli

The green curve (shaded area is standard error) is the mean over all participants for all real trials while the black curve is the same for the pseudotrials. To statistically compare the two curves, the area under the curve (AUC) using the trapezoidal method was computed. This was done from stimulus onset (0ms) to 304ms as it was at 304ms that this mean curve reached 0μV. A Wilcoxon signed rank non-parametric repeated measures test on the AUC was done and found a significant difference between the real and pseudotrials ($Z = 3.659$, $p = 2.536 \times 10^{-4}$). Therefore, this visualization and statistically significant difference confirms a neural response to the no-report sensory stimuli.

5.2.5. Stimulus-responsive contact classification

From the preprocessed data, a high-pass two-way zero-phase FIR filter was applied at 70Hz. This left the signal with high frequency band (HFB) gamma between 70-180Hz. The data was then epoched from -2000ms to 2000ms, with a baseline of -200 to 0ms applied to ERP analysis (Helfrich et al., 2018).

We determined which contacts were stimulus responsive according to the methods of Helfrich (Helfrich et al., 2018). Briefly, a contact was excluded from all subsequent analyses when the average HFB response to the stimulus was below a z-score of ± 1.5 for 10% (50 samples) of consecutive timepoints between stimulus onset (0 ms) and 500 ms (median = 125 ± 37, range = 45–182 contacts removed per participant).

5.2.6. Event-related potentials (ERPs)

Event-related potentials (ERPs) were calculated to confirm a response to the stimuli (or its absence in pseudotrials) and for control analysis (see below). As for all other analyses, the data was epoched from -2000 ms to 2000 ms and was baseline corrected from -200 to 0 ms. The mean of all trials (180) over all contacts was calculated for each participant.

5.2.7. TTV in different frequency bands

The frequencies of the sEEG between 0.1 and 70 Hz was selected as the broadband for TTV calculation. Moreover, the continuous signal was decomposed into the following frequency bands using a two-way zero-phase FIR filter: theta = 4–8 Hz, alpha = 8–13 Hz, beta = 13–30 Hz, low gamma = 30–70 Hz, and high gamma = 70–180 Hz. Afterwards, the filtered signals were epoched. The prestimulus SD, including the median split and high/low grouping, and TTV was computed (as explained above) for each band according to the findings of previous studies (Arazi et al., 2017b; Wolff et al., 2019c). Thus, the filtering of the data was done prior to epoching, and the determination of prestimulus high/low SD groups was done separately for each band.

5.2.8. Real and pseudotrial TTV

The TTV as calculated above includes both a) the effect of the stimulus on the ongoing variability, and b) the ongoing variability that transfers from the prestimulus interval to the poststimulus period (see Eq. 3 below). To disentangle stimulus-related effects within TTV from those of the ongoing variability, we calculated 'pseudotrials' (Huang et al., 2017; Wolff et al., 2019c). Based on fluctuations of the spontaneous activity, the pseudotrials were selected from the ITI preceding each stimulus; specifically, we marked -1500ms (1500ms before onset of the real stimulus) as the virtual stimulus onset and investigated the subsequent 800ms (same duration as the real trials) period as the pseudotrial. In contrast, the real trials were defined as 0 to 800ms of the stimulus-related epoch.

Both real and pseudotrial TTV were calculated in the same way as described above (Results, Eq. 1). To determine if the prestimulus variability had a significant effect on the poststim TTV, the AUC between 450-550ms was calculated using the MATLAB function *trapz* which employs the trapezoidal method of integration.

5.3. EEG data and preprocessing for replication

5.3.1. EEG paradigm

To replicate the findings in the sEEG data, the same analyses were done in a separate dataset with a moral judgement task (Wolff et al., 2019b) (20 participants, 11 females, mean age = 29.9 ± 11.3 years, range of 19–55 years) in scalp EEG. The data was recorded on Neuroscan's 64 channel Quik-Cap with parameters detailed previously (Wolff et al., 2019b). Written informed consent was obtained from all participants prior to participation (REB# 2009018, University of Ottawa Institute of Mental Health Research).

The task employed here was the externally-guided decision-making control task explained in detail elsewhere (Wolff et al., 2019c, 2019b). Briefly, participants were presented with a black screen divided vertically by a white line. On either side of the center line, two-dimensional stick people were presented, with the numbers on either side varying. Each stimulus contained a total of twelve people, however the ratio between the left and right sides differed and was presented for two seconds. The ITI's were jittered at 5 s, 5.5 s and 6s and randomized. The participants' task was to judge whether there were more people on the left side of the screen than the right side. Each participant was presented with four stimuli repeated 45 times each, therefore 180 trials in total, the same number as in the sEEG task.

Participants responded by a button press (the YES button was counterbalanced across participants) with the mean reaction time being 761 $\pm$ 198ms and a range of 391 to 1111ms.

5.3.2. EEG preprocessing and pseudotrial insertion

Preprocessing of the data was done according to standard steps for task-related EEG data (Wolff et al., 2019c, 2019a). The preprocessing for the EEG data was done in MATLAB (The MathWorks, v2018b) with the Optimization, Statistics and Signal Processing Toolboxes using EEGLAB (Delorme and Makeig, 2004) version 14.

To begin, data was resampled to 500 Hz using EEGLAB's *resample* anti-aliasing function. The data was then low- and high-pass filtered using a two-way zero-phase FIR filter at 0.5 Hz and 70 Hz respectively (High Gamma was excluded). Data were then visually inspected. Channels flat longer than 5s, those that had less than 0.8 correlation with neighboring channels or line noise ±4SD compared to other channels were removed (mode = 2, range 0 to 3). The data was then referenced to the average of all channels, as was done in the sEEG preprocessing. To remove 60Hz electrical noise activity, EEGLAB function CleanLine, which uses a multi-taper sliding window approach to remove electrical line noise, was used.

Data was epoched similarly to the sEEG data (described above) and independent component analysis (ICA) reduced stationary artifacts with the Multiple Artifact Rejection Algorithm (Winkler et al., 2014, 2011).

Identical to methods previously stated (Wolff et al., 2019c), pseudotrials were inserted into the EEG blocks. This was done in the ITI preceding the real stimulus, specifically the onset of the pseudotrial was set 3.5s prior to the onset of the actual stimulus. This allowed for a minimum of 1s between the pseudo and real trial.

5.3.3. Reaction time data and behavioral relevance

To determine if there was a significant difference in reaction time between trials with prestimulus high or low variability, the prestimulus SD of trials were split into three groups (triple-split). The corresponding reaction times from the top and bottom third (ascending SD values 1–60 and 121–180) for each frequency band were then extracted and the mean of each group was computed. A repeated measures *t*-test was done for each frequency band to compare the mean reaction times between the low and high prestim.

To correlate the TTV AUC in the difference curves described above (TTV real trials minus TTV pseudotrials), the reaction times for the median split based on the prestimulus SD were extracted and the mean was computed. A two-tailed Spearman's correlation (some of the distributions were non-normal) between these mean reaction times and the TTV AUC was done for both the prestimulus high and low. To support this correlation, a linear polynomial curve was fit to the data using MATLAB v2018b's *fit* function (fitType = 'poly1'). Finally, to contrast these results with those from the TTV curves that were not corrected for prestimulus variability, the same analysis was done with the TTV AUC from the real trials.

5.4. Correlation and statistics

All statistics were computed either in SPSS v24 or MATLAB v2018b using the Statistics Toolbox, and the significance level for all tests was .05. To control for multiple comparisons, the False Discovery Rate by Benjamini-Hochberg Benjamini and Hochberg (1995) was applied to the *p*-values of all statistical tests (See the result sections for more detailed statistics).

Repeated measures *t*-tests and ANOVA's were used as all participants contributed to both/all levels (real trials/corrected trials/pseudotrials, prestimulus low/prestimulus high, etc). All assumptions of ANOVA's were met prior to calculating the statistical test.

Declaration of Competing Interest

The authors declare no competing interests.

Acknowledgments

This work was supported by the EJLB-Michael Smith Foundation, the Canadian Institutes of Health Research, the Ministry of Science and Technology of China, the National Key R&D Program of China (2016YFC1306700), the Hope of Depression Foundation (HDRF), and the Start-Up Research Grant in Hangzhou Normal University (to Georg Northoff). This research has also received funding from the European Union's Horizon 2020 Framework Program for Research and Innovation under the Specific Grant Agreement No. 785907 (Human Brain Project SGA2).

Author Contributions

LC, SJ, JH, and YM acquired the sEEG data, while YM was responsible for overseeing the patient recruitment and data acquisition. AW, ST and GN conceived of the idea of the study, AW and ST did the preprocessing and analysis of the sEEG data, and AL provided feedback and suggested further analyses. AW acquired and analyzed the EEG replication data. AW and GN wrote the manuscript, while ST, JGP and AL edited the manuscript and made suggestions.

Credit_author_statement

Annemarie Wolff: Conceptualization, Methodology, Formal analysis, Visualization, Writing.

Liang Chen: Data curation, Resources.

Shankar Tumati: Conceptualization, Methodology, Writing – review and editing.

Mehrshad Golesorkhi: Conceptualization, formal analysis, Writing – review and editing.

Javier Gomez-Pilar: formal analysis, Writing – review and editing.

Jie Hu: Data curation, Resources.

Shize Jiang: Data curation, Resources.

Ying Mao: Resources, Funding acquisition.

Andre Longtin: formal analysis, Writing – review and editing.

Georg Northoff: Conceptualization, Resources, Funding acquisition, Writing.

Data and Code Availability

The data used in this manuscript is not publicly available due to confidentiality and privacy issues of data from a clinical (neurologic) population, according to the guidelines of the relevant Research Ethics Board.

All MATLAB code and functions used in the analysis for this paper are available upon request to the corresponding author (A Wolff).

Supplementary materials

Supplementary material associated with this article can be found, in the online version, at doi:10.1016/j.neuroimage.2021.118160.

References

Arazi, A., Censor, N., Dinstein, I., 2017a. Neural variability quenching predicts individual perceptual abilities. J. Neurosci. 37, 97–109. doi:10.1523/JNEUROSCI.1671-16.2017.

Arazi, A., Gonen-Yaacovi, G., Dinstein, I., 2017b. The magnitude of trial-by-trial neural variability is reproducible over time and across tasks in humans. eNeuro 4, 0292. doi:10.1523/ENEURO.0292-17.2017, –17. 2017.

Arieli, A., Sterkin, A., Grinvald, A., Aertsen, A., 1996. Dynamics of ongoing activity: explanation of the large variability in evoked cortical responses. Science 273 (80-.), 1868–1871.

Baria, A.T., Maniscalco, B., He, B.J., 2017. Initial-state-dependent, robust, transient neural dynamics encode conscious visual perception. PLoS Comput. Biol. 13, 1–29. doi:10.1371/journal.pcbi.1005806.

Benjamini, Y., Hochberg, Y., 1995. Controlling the false discovery rate : a practical and powerful approach to multiple testing. J. R. Stat. Soc. 57, 289–300.

Benwell, C.S.Y., Tagliabue, C.F., Veniero, D., Cecere, R., Savazzi, S., Thut, G., 2017. Prestimulus EEG power predicts conscious awareness but not objective visual performance. eNeuro 4. doi:10.1523/ENEURO.0182-17.2017, ENEURO.0182-17.2017.

Buzsáki, G., Anastassiou, C.A., Koch, C., 2012. The origin of extracellular fields and currents-EEG, ECoG, LFP and spikes. Nat. Rev. Neurosci. 13, 407–420. doi:10.1038/nrn3241.

Cao, L., Thut, G., Gross, J., 2017. The role of brain oscillations in predicting self-generated sounds. Neuroimage 147, 895–903. doi:10.1016/j.neuroimage.2016.11.001.

Chang, M.H., Armstrong, K.M., Moore, T., 2012. Dissociation of response variability from firing rate effects in frontal eye field neurons during visual stimulation, working memory, and attention. J. Neurosci. 32, 2204–2216. doi:10.1523/JNEUROSCI.2967-11.2012.

Churchland, A.K., Kiani, R., Chaudhuri, R., Wang, X.J., Pouget, A., Shadlen, M.N., 2011. Variance as a signature of neural computations during decision making. Neuron 69, 818–831. doi:10.1016/j.neuron.2010.12.037.

Churchland, M.M., Yu, B.M., Cunningham, J.P., Sugrue, L.P., Cohen, M.R., Corrado, G.S., Newsome, W.T., Clark, A.M., Hosseini, P., Scott, B.B., Bradley, D.C., Smith, M.A., Kohn, A., Movshon, J.A., Armstrong, K.M., Moore, T., Chang, S.W., Snyder, L.H., Lisberger, S.G., Priebe, N.J., Finn, I.M., Ferster, D., Ryu, S.I., Santhanam, G., Sahani, M., Shenoy, K.V., 2010. Stimulus onset quenches neural variability: a widespread cortical phenomenon. Nat. Neurosci. 13, 369–378. doi:10.1038/nn.2501.

Curto, C., Sakata, S., Marguet, S., Itskov, V., Harris, K.D., 2009. A simple model of cortical dynamics explains variability and state dependence of sensory responses in urethane-anesthetized auditory cortex. J. Neurosci. 29, 10600–10612. doi:10.1523/jneurosci.2053-09.2009.

Daitch, A.L., Parvizi, J., 2018. Spatial and temporal heterogeneity of neural responses in human posteromedial cortex. Proc. Natl. Acad. Sci doi:10.1073/pnas.1721714115, 201721714.

Daniel, E., Meindert, T., Arazi, A., Donner, T.H., Dinstein, I., 2019. The relationship between trial-by- trial variability and oscillations of cortical population activity. Sci. Rep 1–11. doi:10.1038/s41598-019-53270-7.

Delorme, A., Makeig, S., 2004. EEGLAB: an open source toolbox for analysis of single-trial EEG dynamics. J. Neurosci. Methods 134, 9–21.

Dinstein, I., Heeger, D.J., Behrmann, M., 2015. Neural variability: friend or foe? Trends Cogn. Sci. 19, 322–328. doi:10.1016/j.tics.2015.04.005.

Fellinger, R., Klimesch, W., Gruber, W., Freunberger, R., Doppelmayr, M., 2011. Prestimulus alpha phase-alignment predicts P1-amplitude. Brain Res. Bull. 85, 417–423. doi:10.1016/j.brainresbull.2011.03.025.

Ferri, F., Costantini, M., Huang, Z., Perrucci, M.G., Ferretti, A., Romani, G.L., Northoff, G., 2015. Intertrial variability in the premotor cortex accounts for individual differences in peripersonal space. J. Neurosci. 35, 16328–16339. doi:10.1523/JNEUROSCI.1696-15.2015.

Finn, I.M., Priebe, N.J., Ferster, D., 2007. The emergence of contrast-invariant orientation tuning in simple cells of cat visual cortex. Neuron 54, 137–152. doi:10.1016/j.neuron.2007.02.029.

Friston, K.J., 2010. The free-energy principle: a unified brain theory? Nat. Rev. Neurosci. 11, 127–138. doi:10.1038/nrn2787.

Galindo-Leon, E.E., Stitt, I., Pieper, F., Stieglitz, T., Engler, G., Engel, A.K., 2019. Context-specific modulation of intrinsic coupling modes shapes multisensory processing. Sci. Adv. 5, 1–12. doi:10.1126/sciadv.aar7633.

Garrett, D.D., Samanez-Larkin, G.R., MacDonald, S.W.S., Lindenberger, U., McIntosh, A.R., Grady, C.L., 2013. Moment-to-moment brain signal variability: a next frontier in human brain mapping? Neurosci. Biobehav. Rev. 37, 610–624. doi:10.1016/j.neubiorev.2013.02.015.

Gonzalez-Martinez, J.A., 2016. The stereo-electroencephalography: the epileptogenic zone. J. Clin. Neurophysiol. 33, 522–529. doi:10.1097/WNP.0000000000000327.

Goris, R., Movshon, J.A., Simoncelli, E., 2014. Partitioning neuronal variability. Nat. Neurosci. 18, 386–392. doi:10.1038/nn.3945.Dopaminergic.

Groot, J.M., Boayue, N.M., Csifcsák, G., Boekel, W., Huster, R., Forstmann, B.U., Mittner, M., 2021. Probing the neural signature of mind wandering with simultaneous fMRI-EEG and pupillometry. Neuroimage 224. doi:10.1016/j.neuroimage.2020.117412.

Gulbinaite, R., van Viegen, T., Wieling, M., Cohen, M.X., VanRullen, R., 2017. Individual alpha peak frequency predicts 10 hz flicker effects on selective attention. J. Neurosci. 37, 10173–10184. doi:10.1523/jneurosci.1163-17.2017.

Haar, S., Donchin, O., Dinstein, I., 2017. Individual movement variability magnitudes are explained by cortical neural variability. J. Neurosci. 37, 9076–9085. doi:10.1523/JNEUROSCI.1650-17.2017.

Hanslmayr, S., Volberg, G., Wimber, M., Dalal, S.S., Greenlee, M.W., 2013. Prestimulus oscillatory phase at 7 Hz gates cortical information flow and visual perception. Curr. Biol. 23, 2273–2278. doi:10.1016/j.cub.2013.09.020.

He, B.J., 2013. Spontaneous and task-evoked brain activity negatively interact. J. Neurosci. 33, 4672–4682. doi:10.1523/JNEUROSCI.2922-12.2013.

He, B.J., Snyder, A.Z., Zempel, J.M., Smyth, M.D., Raichle, M.E., 2008. Electrophysiological correlates of the brain's intrinsic large-scale functional architecture. Proc. Natl. Acad. Sci. 105, 16039–16044. doi:10.1073/pnas.0807010105.

He, B.J., Zempel, J.M., 2013. Average is optimal: an inverted-u relationship between trial-to-trial brain activity and behavioral performance. PLoS Comput. Biol. 9. doi:10.1371/journal.pcbi.1003348.

Helfrich, R.F., Fiebelkorn, I.C., Szczepanski, S.M., Lin, J.J., Parvizi, J., Knight, R.T., Kastner, S., 2018. Neural mechanisms of sustained attention are rhythmic. Neuron 99, 854–865.e5. doi:10.1016/j.neuron.2018.07.032.

Hennequin, G., Ahmadian, Y., Rubin, D.B., Lengyel, M., Miller, K.D., 2018. The dynamical regime of sensory cortex: stable dynamics around a single stimulus-tuned attractor account for patterns of noise variability. Neuron 98, 846–860.e5. doi:10.1016/j.neuron.2018.04.017.

Hirschmann, J., Baillet, S., Woolrich, M., Schnitzler, A., Vidaurre, D., Florin, E., 2019. Spontaneous network activity <35 Hz accounts for variability in stimulus-induced gamma responses. Neuroimage, 116374 doi:10.1016/J.NEUROIMAGE.2019.116374.

Huang, C., Ruff, D.A., Pyle, R., Rosenbaum, R., Cohen, M.R., Doiron, B., 2019. Circuit models of low-dimensional shared variability in cortical networks. Neuron 101, 337–348.e4. doi:10.1016/j.neuron.2018.11.034.

Huang, Z., Zhang, J., Longtin, A., Dumont, G., Duncan, N.W., Pokorny, J., Qin, P., Dai, R., Ferri, F., Weng, X., Northoff, G., 2017. Is there a nonadditive interaction between spontaneous and evoked activity? phase-dependence and its relation to the temporal structure of scale-free brain activity. Cereb. Cortex 27, 1–23. doi:10.1093/cercor/bhv288.

Huang, Z., Zhang, Jun, Wu, J., Liu, X., Xu, J., Zhang, Jianfeng, Qin, P., Dai, R., Yang, Z., Mao, Y., Hudetz, A.G., Northoff, G., 2018. Disrupted neural variability during propofol-induced sedation and unconsciousness. Hum. Brain Mapp. 39, 1–12. doi:10.1002/hbm.24304.

Huk, A., Bonnen, K., He, B.J., 2018. Beyond trial-based paradigms: Continuous behavior, ongoing neural activity, and natural stimuli. J. Neurosci. 38, 1920. doi:10.1523/JNEUROSCI.1920-17.2018, –17.

Hussar, C., Pasternak, T., 2010. Trial-to-trial variability of the prefrontal neurons reveals the nature of their engagement in a motion discrimination task. Proc. Natl. Acad. Sci 107, 21842–21847. doi:10.1073/pnas.1009956107.

Kisley, M.a., Gerstein, G.L., 1999. Trial-to-trial variability and state-dependent modulation of auditory-evoked responses in cortex. J. Neurosci. 19, 10451–10460. doi:10.1523/JNEUROSCI.19-23-10451.1999.

Lin, I.C., Okun, M., Carandini, M., Harris, K.D., 2015. The nature of shared cortical variability. Neuron 87, 645–657. doi:10.1016/j.neuron.2015.06.035.

Lipsman, N., Nakao, T., Kanayama, N., Krauss, J.K., Anderson, A., Giacobbe, P., Hamani, C., Hutchison, W.D., Dostrovsky, J.O., Womelsdorf, T., Lozano, A.M., Northoff, G., 2014. Neural overlap between resting state and self-relevant activity in human subcallosal cingulate cortex - Single unit recording in an intracranial study. Cortex 60, 139–144. doi:10.1016/j.cortex.2014.09.008.

Liu, X., Zhang, C., Ji, Z., Ma, Y., Shang, X., Zhang, Q., Zheng, W., Li, X., Gao, J., Wang, R., Wang, J., Yu, H., 2016. Multiple characteristics analysis of Alzheimer's electroencephalogram by power spectral density and Lempel–Ziv complexity. Cogn. Neurodyn. 10, 121–133. doi:10.1007/s11571-015-9367-8.

Luczak, A., Bartho, P., Harris, K.D., 2013. Gating of sensory input by spontaneous cortical activity. J. Neurosci. 33, 1684–1695. doi:10.1523/jneurosci.2928-12.2013.

Madore, K.P., Khazenzon, A.M., Backes, C.W., Jiang, J., Uncapher, M.R., Norcia, A.M., Wagner, A.D., 2020. Memory failure predicted by attention lapsing and media multitasking. Nature 587, 87–91. doi:10.1038/s41586-020-2870-z.

Mathewson, K.E., Gratton, G., Fabiani, M., Beck, D.M., Ro, T., 2009. To see or not to see: prestimulus alpha phase predicts visual awareness. J. Neurosci. 29, 2725–2732. doi:10.1523/JNEUROSCI.3963-08.2009.

Mazzucato, L., Fontanini, A., La Camera, G., 2016. Stimuli reduce the dimensionality of cortical activity. Front. Syst. Neurosci. 10. doi:10.3389/fnsys.2016.00011.

Mazzucato, L., Fontanini, A., La Camera, G., 2015. Dynamics of multi-stable states during ongoing and evoked cortical activity. J Neurosci 35, 8214–8231. doi:10.1523/JNEUROSCI.4819-14.2015.

Milton, A., Pleydell-Pearce, C.W., 2016. The phase of pre-stimulus alpha oscillations influences the visual perception of stimulus timing. Neuroimage 133, 53–61. doi:10.1016/j.neuroimage.2016.02.065.

Monier, C., Chavane, F., Baudot, P., Graham, L.J., Frégnac, Y., 2003. Orientation and direction selectivity of synaptic inputs in visual cortical neurons: a diversity of combinations produces spike tuning. Neuron 37, 663–680. doi:10.1016/S0896-6273(03)00064-3.

Nieus, T., D'Andrea, V., Amin, H., Di Marco, S., Safaai, H., Maccione, A., Berdondini, L., Panzeri, S., 2018. State-dependent representation of stimulus-evoked activity in high-density recordings of neural cultures. Sci. Rep. 8, 1–19. doi:10.1038/s41598-018-23853-x.

Northoff, G., Qin, P., Nakao, T., 2010. Rest-stimulus interaction in the brain: a review. Trends Neurosci 33, 277–284. doi:10.1016/j.tins.2010.02.006.

Pachitariu, M., Lyamzin, D.R., Sahani, M., Lesica, N.a., 2015. State-dependent population coding in primary auditory cortex. J. Neurosci. 35, 2058–2073. doi:10.1523/JNEUROSCI.3318-14.2015.

Parvizi, J., Kastner, S., 2018. Promises and limitations of human intracranial electroencephalography. Nat. Neurosci. 21, 474–483. doi:10.1038/s41593-018-0108-2.

Podvalny, E., Flounders, M.W., King, L.E., Holroyd, T., He, B.J., 2019. A dual role of prestimulus spontaneous neural activity in visual object recognition. Nat. Commun. 10, 1–13. doi:10.1038/s41467-019-11877-4.

Qin, C., Tan, Z., Pan, Y., Li, Y., Wang, Lin, Ren, L., Zhou, W., Wang, Liang, 2017. Automatic and precise localization and cortical labeling of subdural and depth intracranial electrodes. Front. Neuroinform. 11, 1–10. doi:10.3389/fninf.2017.00010.

Qin, P., Liu, Y., Shi, J., Wang, Y., Duncan, N.W., Gong, Q., Weng, X., Northoff, G., 2012. Dissociation between anterior and posterior cortical regions during self-specificity and familiarity: a combined fMRI-meta-analytic study. Hum. Brain Mapp. 33, 154–164. doi:10.1002/hbm.21201.

Romei, V., Brodbeck, V., Michel, C., Amedi, A., Pascual-Leone, A., Thut, G., 2008. Spontaneous fluctuations in posterior α-band EEG activity reflect variability in excitability of human visual areas. Cereb. Cortex 18. doi:10.1093/cercor/bhm229, 2010–2018.

Scaglione, A., Moxon, K.A., Aguilar, J., Foffani, G., 2011. Trial-to-trial variability in the responses of neurons carries information about stimulus location in the rat whisker thalamus. Proc. Natl. Acad. Sci. 108, 14956–14961. doi:10.1073/pnas.1103168108.

Scholvinck, M.L., Saleem, A.B., Benucci, A., Harris, K.D., Carandini, M., 2015. Cortical state determines global variability and correlations in visual cortex. J. Neurosci. 35, 170–178. doi:10.1523/jneurosci.4994-13.2015.

Schurger, A., Pereira, F., Treisman, A., Cohen, J.D., 2010. Reproducibility distinguishes

conscious from nonconscious neural representations. Science 327 (80-.), 97–99. doi:10.1016/j.neuropsychologia.2008.12.029.Predicting.

Schurger, A., Sarigiannidis, I., Naccache, L., Sitt, J.D., Dehaene, S., 2015. Cortical activity is more stable when sensory stimuli are consciously perceived. Proc. Natl. Acad. Sci. 112, E2083–E2092. doi:10.1073/pnas.1418730112.

Shimaoka, D., Steinmetz, N.A., Harris, K.D., Carandini, M., 2019. The impact of bilateral ongoing activity on evoked responses in mouse cortex. Elife 8, 1–19. doi:10.7554/eLife.43533.

Tsuchiya, N., Wilke, M., Frässle, S., Lamme, V.A.F., 2015. No-report paradigms: extracting the true neural correlates of consciousness. Trends Cogn. Sci. 19, 757–770. doi:10.1016/j.tics.2015.10.002.

Waschke, L., Kloosterman, N.A., Obleser, J., Garrett, D.D., 2021. Behavior needs neural variability. Neuron 1–16. doi:10.1016/j.neuron.2021.01.023.

White, B., Abbott, L.F., Fiser, J., 2012. Suppression of cortical neural variability is stimulus- and state-dependent. J. Neurophysiol. 108, 2383–2392. doi:10.1152/jn.00723.2011.

Winkler, I., Brandl, S., Horn, F., Waldburger, E., Allefeld, C., Tangermann, M., 2014. Robust artifactual independent component classification for BCI practitioners. J. Neural Eng. 11. doi:10.1088/1741-2560/11/3/035013.

Winkler, I., Haufe, S., Tangermann, M., 2011. Automatic classification of artifactual ica- components for artifact removal in EEG signals. Behav. Brain Funct. 7, 30. doi:10.1186/1744-9081-7-30.

Wolff, A., de la Salle, S., Sorgini, A., Lynn, E., Blier, P., Knott, V., Northoff, G., 2019a. Atypical temporal dynamics of resting state shapes stimulus- evoked activity in depression — an EEG study on rest – stimulus interaction. Front. Psychiatry 10, 1–16. doi:10.3389/fpsyt.2019.00719.

Wolff, A., Gomez-Pilar, J., Nakao, T., Northoff, G., 2019b. Interindividual neural differences in moral decision-making are mediated by alpha power and delta/theta phase coherence. Sci. Rep. 9, 1–13. doi:10.1038/s41598-019-40743-y.

Wolff, A., Yao, L., Gomez-Pilar, J., Shoaren, M., Jiang, N., Northoff, G., 2019c. Neural variability quenching during decision-making: neural individuality and its prestimulus complexity. Neuroimage 192, 1–14.

Yamagishi, N., Callan, D.E., Anderson, S.J., Kawato, M., 2008. Attentional changes in prestimulus oscillatory activity within early visual cortex are predictive of human visual performance. Brain Res 1197, 115–122. doi:10.1016/j.brainres.2007.12.063.